CRATER LAKE, OREGON

Measurements of spectral optical properties and their relation to biogeochemical variables and processes in Crater Lake, Crater Lake National Park, OR

Emmanuel S. Boss · Robert Collier · Gary Larson · Katja Fennel · W. S. Pegau

Abstract Spectral inherent optical properties (IOPs) have been measured at Crater Lake, OR, an extremely clear sub-alpine lake. Indeed Pure water IOPs are major contributors to the total IOPs, and thus to the color of the lake. Variations in the spatial distribution of IOPs were observed in June and September 2001, and reflect biogeochemical processes in the lake. Absorption by colored dissolved organic material increases with depth and between June and September in the upper 300 m. This pattern is consistent with a net release of dissolved organic materials from primary and secondary production through the summer and its photo-oxidation near the surface. Waters fed by a tributary near the lake's rim exhibited low levels of absorption by dissolved organic materials. Scattering is mostly dominated by organic particulate material, though inorganic material is found to enter the lake from the rim following a rain storm. Several similarities to oceanic oligotrophic regions are observed: (a) The Beam attenuation correlates well with particulate organic material (POM) and the relationship is similar to that observed in the open ocean. (b) The specific absorption of colored dissolved organic material has a value similar to that of open ocean humic material. (c) The distribution of chlorophyll with depth does not follow the distribution of particulate organic material due to photo-acclimation resulting in a subsurface pigment maximum located about 50 m below the POM maximum.

Keywords Crater Lake · Optics · Biogeochemistry · Backscattering coefficient

E. S. Boss (✉)
University of Maine, 5741 Libby Hall, Orono, ME 04469, USA
e-mail: emmanuel.boss@maine.edu

R. Collier · W. S. Pegau
Oregon State University, COAS, 104 Ocean. Admin. Bldg., Corvallis, OR 97331, USA

G. Larson
USGS Forest and Rangeland Ecosystem Science Center, 3200 Jefferson Way, Corvallis, OR 97331, USA

K. Fennel
IMCS, Rutgers University, 71 Dudley Road, New Brunswick, NJ 08901, USA

Introduction

Novel commercial in-situ spectral optical instrumentation, developed in the past decade, has opened oceans and lakes to exploration of

biogeochemical processes at sub-1 m scales, scales, which have not been accessible previously. From a data poor field, with only a handful of absorption spectra measured per water column, hydrological optics has become a data rich field with spectra generated at sub-Hz and thus at sub-1 m resolution. Until the recent development of a commercial in-situ spectral absorption and attenuation sensor (Moore et al., 1997) and backscattering sensors (Maffione & Dana, 1997; Zaneveld et al., 2003), absorption and backscattering were not measured in high resolution, routinely, and in-situ.

The absorption and backscattering coefficients are important inherent optical properties, in particular since they are tightly linked to the color of a water body (e.g., Gordon et al., 1988). The link between the color of a water body and its inherent optical properties (properties not affected by the illumination conditions such as absorption, scattering, and attenuation, hereafter IOP) is provided by the radiative-transfer equation (e.g., Mobley, 1994); knowledge of the IOP and the illumination conditions is sufficient to predict the color of the lake that will be perceived by an observer.

IOP are routinely inverted to provide information about the concentration and nature of the particulates and dissolved substances in aquatic environments. Inversions of IOP have been used to estimate the volume of total suspended matter from beam attenuation (Spinrad & Zaneveld, 1982), particulate organic matter concentration from beam attenuation (Bishop, 1999), dissolved organic matter concentration from absorption by dissolved material (e.g., review by Blough & Green, 1995), chlorophyll concentration from fluorescence or particulate absorption, particulate size distribution from spectral particulate beam attenuation (Boss et al., 2001a), and bulk particulate composition from the particulate backscattering ratio (Twardowski et al., 2001; Boss et al., 2004).

Measurements of IOP in lakes have mostly been limited to single-beam transmissometers and land-based spectrophotometry (e.g., review by Bukata et al., 1995). In this paper we present data of spectral IOP measured in-situ in Crater Lake, OR.

Crater Lake is a sub-alpine lake (Altitude 1,883 m), 589 m deep (deepest in the US), and enclosed by a volcano's caldera with a radius of nearly 3 km at the lake's surface (Klimasauskas et al., 2002). Crater Lake has been a natural laboratory for hydrological optics for nearly 70 years. Pettit (1936) performed measurements of spectral backscattering there and found them to be comparable to distilled water. Smith & Baker (1981) used it as part of their dataset to determine the absorption of the clearest natural waters. In this paper we present the first *spectral* IOP measurements in Crater Lake. The clarity of Crater Lake provides a challenge to the novel spectral IOP instrumentation, since the signal is very weak. If this instrumentation is found to work satisfactorily at Crater Lake, it is likely to perform well in most natural conditions (assuming that the path-length is reduced in very turbid waters).

Material and methods

Sampling

Data were collected during two sampling periods. In June 2001 we sampled following a rain storm. We sampled at two stations in the lake. Sta. 13, over the deepest area of the lake (42°56′ N, 122°06′ W), was sampled on two consecutive days (June 28–29) down to 300 m depth (a subset of these data was analyzed in Fennel & Boss, 2003). On June 28 we also sampled a shallow (6 m) station where a turbid whitish stream of water flowed into the lake from the caldera walls. We returned to Sta. 13 on September 19th and sampled to within 20 m of the lake's bottom (596 m).

Data collection and method of analysis

Spectral absorption and attenuation, hydrographic properties and spectral backscattering were measured on a winched package with a single WETLabs' ac-9, a SeaBird SBE25 and a HobiLabs Hydroscat-6 (HS-6), respectively. Additionally, a WETLabs' Eco-VSF was used to measure backscattering in September.

Chlorophyll fluorescence was measured with a WETLabs WetStar. At each station two repeated casts were taken, one of which had 0.2 μm filters (Gelman Suporcap 100) one attached to each intakes of the absorption, and attenuation tubes of the ac-9 for the measurements of CDM absorption (Colored Dissolved Material, operationally material that goes through a 0.2 μm filter). In September we also used a 1 μm filter (Whatman Capsule) at each intake of the ac-9. New filters were used for each field campaign.

Data were binned to 1 m bins by computing the median of the properties in that bin. Particulate properties were computed by subtracting the binned measurement in a vertical profile of spectral absorption and attenuation with the 0.2 μm pre-filter from a profile performed without a filter. Some errors may be caused by the temporal departure between the two measurements (approximately 30 min), given the presence of internal waves confirmed in temperature profiles. However, these departures are likely to result in small uncertainties in the derived particulate absorption and attenuation due to the slowly varying profile of CDM with depth (see below). Note that differences between two successive measurements, with and without filter, result in a particulate profile that is independent of the instrument calibration (assuming we sample the same waters). Thus the likely errors of the measurements of absorption and attenuation are limited by the precision of the instrument (± 0.001 m^{-1}) and the environmental variability and not the accuracy of the calibration (performed with pure water before and after the cruise at the author's lab following the method of Twardowski et al., 1999). Note that an additional uncertainty may be caused by changes in filter efficiency with use. Consistency of CDM values between consecutive profiles (not shown) suggested that this was not a significant problem during the deployments.

Backscattering by particles with the HS-6 (measures scattering at one angle, centered about a scattering angle of 140°) was computed using the method outlined in Boss & Pegau (2001). The volume scattering function measured (of water and particles) was multiplied by a factor of 1.12 to account for a correction in the calibration factor

due to Spectralon reflectivity that has been detected in Dec. 2002 (D. Dana, personal communication, 2004). Application of this factor resulted in an improved agreement between the different ways of estimating the backscattering coefficient than achieved in Boss et al. (2004) (see below). The Eco-VSF (measures scattering at three angles in the back direction, centered at 100, 125, and 150°) was processed following Zaneveld et al. (2003). We had problems with two wavelengths of the HS-6; the 555-channel was observed to shift values within casts in a manner uncorrelated with the other wavelengths and to have the largest standard deviation during calibration. The 676 nm channel was highly correlated with chlorophyll concentration (probably due to its recording of some chlorophyll fluorescence excited at 676 and emitted at 681 nm), unlike the remaining four channels. We therefore present only four channels (440, 488, 530, 620 nm) of the HS-6 data (Fig. 1).

It is interesting to note that the contribution of molecular backscattering by pure water to the total backscattering coefficient in our measurements (the sum of water and particulate backscattering) varies from nearly 60% to 30%
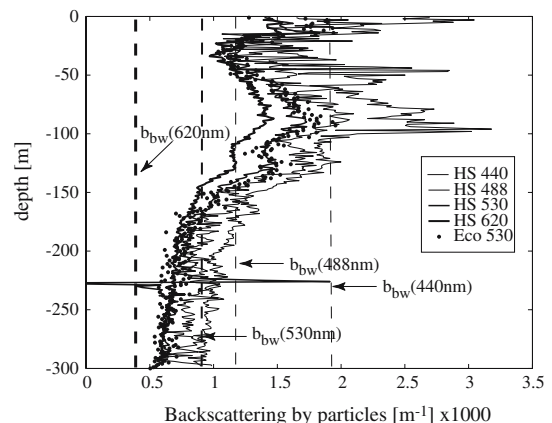

Fig. 1 Vertical distribution of the particulate backscattering coefficient obtained at four wavelengths (HS-6) and at a single wavelength (Eco-VSF) on Sep. 19, 2001 at St. 13. The straight lines, denotes the values of backscattering by pure water based on Morel (1974). The regression between the backscattering coefficients at 530 nm between the measurements by the two backscattering instruments is $b_{bp}(530, \text{EcoVSF}) = 0.97 b_{bp}(530, \text{HS6})$, and the correlation coefficient between them is 0.97. The spike in the HS-6 (530 nm) could not be explained

between blue and red wavelengths at depth (Fig. 1). In the calculation of particulate back-scattering the contribution from water was subtracted out of the total backscattering assuming the backscattering by water to be constant and equal to the values of Morel (1974). The remaining backscattering is attributed to particles as it is customary, to assume a negligible contribution of CDM to scattering and backscattering (e.g., Mobley, 1994).

Chlorophyll concentration was estimated in three ways:

1. Chlorophyll fluorescence (WETLabs Wet-Star) calibrated against chlorophyll estimates from discrete samples analyzed with HPLC.
2. The line-height of the chlorophyll absorption peak in the red: ([chl] = {$a_p(676)$ – ($39/65 \cdot a_p(650)$ + $26/65 \cdot a_p(715)$))}/0.014), e.g., Davis et al. (1997), where a_p denotes particulate absorption, and the wavelength is given in brackets. The value of the chlorophyll-specific absorption, $a^*(676)$ = 0.014 m^2 g chl^{-1} used here is consistent with published literature values for the oceanic assemblages of phytoplankton (e.g., Sosik & Mitchell, 1995) and was chosen here based on regression of HPLC determina-

tion of [chl] versus absorption based [chl]. $a^*(676)$ is likely to vary with depth, as packaging within cells changes its value. Published values of $a^*(676)$ vary from 0.008 m^2 g chl^{-1} to 0.023 m^2 g chl^{-1} (Bricaud et al., 1995; Sosik & Mitchell, 1995).

3. Discrete chlorophyll concentration obtained with HPLC.

The squared correlation coefficient between the chlorophyll fluorescence and absorption is $R^2 = 0.83$ (Fig. 2, $N = 570$). The absorption estimated [chl] has the advantage of not suffering from near-surface non-photochemical quenching which reduces the fluorescence-yield of phytoplankton exposed to high light near the surface. The uncertainty for the absorption-estimated [chl] is ±0.2 μg l^{-1} (~mg m^{-3}) based on the uncertainty in ac-9 measurements (see below, and not taking into account the possible bias in a^* which is likely to add and uncertainty of ±30%). Negative values (~ –0.05 μg l^{-1}) in absorption based chlorophyll estimates observed in Fig. 2 are indicative of too big a removal of the detrital absorption from the particulate absorption in the calculation of phytoplankton absorption at 676 nm. Note that these values are well below the uncertainty in the absorption-based chlorophyll.

Slopes of the particulate size distribution (the "PSD slope") were estimated from the attenuation spectrum by fitting a hyperbolic function to the particulate attenuation spectrum (e.g., Boss et al., 2001a). This method provides an estimate for the broad PSD slope assuming a hyperbolic particulate PSD (see Boss et al., 2001b, for a critical analysis of the assumptions). This method provides an estimate of the spatial changes in the mean particle size. We fitted a similar function to the particulate backscattering spectrum to assess whether there is any relation between this spectrum and that of particulate beam attenuation, and found no significant relation between the two (not shown). If the particles were non-absorbing and the measurements were error free we would have expected the slopes to be similar based on Mie theory (Morel, 1973).

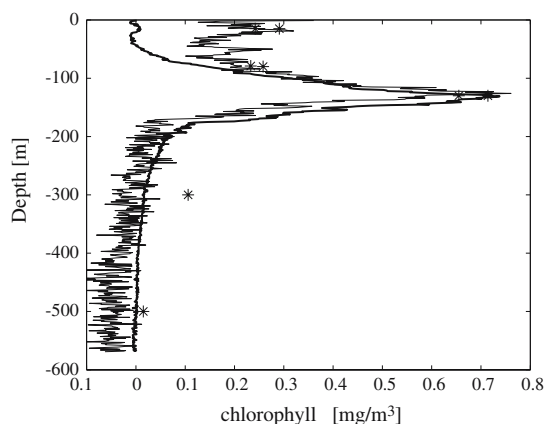Bulk particulate index of refraction was estimated using the method of Twardowski et al.

Fig. 2 Comparison between three estimates of chlorophyll; WetStar fluorometer (bold black line), chlorophyll estimated from particulate absorption line height (black), and HPLC (asterisks) based on measurements at St. 13, Sep. 19, 2001. Note that, unlike fluorescence, the absorption estimate of chlorophyll concentration does not suffer from non-photochemical quenching near the surface

(2001). The bulk index of refraction provides an insight into the particulate composition; phytoplankton and detritus tend to have a low index of refraction ($n = 1.02–1.1$) due to a large water fraction while inorganic particles have a larger index of refraction ($n = 1.12–1.24$) (see Twardowski et al., 2001; Boss et al., 2004, for detailed discussion). Twardowski et al. (2001) developed a method to obtain information on the bulk index of refraction from knowledge of the particulate size distribution and the particulate backscattering ratio (the ratio of particulate backscattering to particulate scattering). Assuming the particulate size distribution (PSD) to be hyperbolic, a relationship has been found between the hyperbolic slope of the PSD and the spectral slope of particulate beam attenuation (e.g., Boss et al., 2001a, and references therein).

Discrete samples for chlorophyll and particulate organic carbon (POC) were collected in September and processed with the same methods as in Urbach et al. (2001). In addition, cells were collected in September for Flow-cytometric analysis.

Uncertainties in measurements

While with calibration, the error of the ac-9 are assumed to be $O(0.005 \text{ m}^{-1})$ (Twardowski et al., 1999) we estimate the particulate absorption and attenuation measurement presented here to be accurate to within $O(0.002 \text{ m}^{-1})$. This is because the values for the particulate attenuation and absorption were measured using a single instrument deployed with and without a pre-filter. Assuming the in-water properties to stay constant between the two consecutive profiles (30 min) the uncertainty is only limited by the instrument precision (0.001 m^{-1}) and stability of the instrument measuring the same waters $O(0.002 \text{ m}^{-1})$. Note that changes in filter efficiency with time would increase these uncertainties. As noted above, we have not noticed changes in CDM concentration at depth between consecutive profiles, indicating no noticeable change in filter performance.

Note, however, that to this date there is a large uncertainty in the particulate absorption in the blue region of the spectrum due to issues associated with the scattering correction of particulate absorption. Different methods of the ''Scattering correction'' (e.g., Zaneveld et al., 1994) deviate by up to 20% in their estimate of absorption in the blue, while converging towards the red part of the spectrum. The scattering correction method used here was method 3 of Zaneveld et al. (1994), in which a fixed portion of scattering is removed from the measured absorption. The proportion of scattering that is removed equals the measured ratio of absorption and scattering at 715 nm, consistent with assuming zero absorption by particles at 715 nm. Uncertainty in colored dissolved material absorption (CDM) is 0.005 m^{-1}, a sizable uncertainty relative to the absolute CDM absorption measured in Crater Lake. To reduce this uncertainty the two independent measurements of CDM absorption obtained by the a- and c-sides of the ac-9 were averaged, reducing the uncertainty to 0.0035 m^{-1}.

Backscattering errors are assumed to be smaller than 15% of the signal based on uncertainties in converting light backscattered at 140 to the backscattering coefficient (Maffione & Dana, 1997; Boss et al., 2004). An additional uncertainty based on variability in the instruments' calibration history is $\pm 0.0002 \text{ m}^{-1}$ (D. Dana, 2004, personal communication). Comparison of particulate backscattering estimates at 530 nm based on the two backscattering instruments reveals that the two are highly correlated ($R^2 = 0.94$, $N = 298$), with the Eco-VSF being on average 0.97 times the HS-6 and with an offset that is not significantly different from zero (Fig. 1). This is an excellent agreement, in particular given that the two instruments are calibrated differently and that the backscattering coefficient is computed differently from each measurement (Zaneveld et al., 2003). It also indicates that the uncertainties quoted above are probably too conservative.

Uncertainties in the particulate backscattering ratio, the ratio of backscattering to total scattering, are likely to be less than 20%, based on propagating the errors of scattering and backscattering. Uncertainties in the discrete measurements were estimated from replicate samples and are 0.05 mg l^{-1} for chlorophyll and nearly 30% for POC.

Fig. 3 Measurements of temperature, particulate attenuation at 650 nm, and chlorophyll (absorption based) as function of depth (top row) and of particulate attenuation at 650 nm, and chlorophyll as function of temperature (bottom row). Measurements were taken at St. 13 on June 28 (thin) and June 29 (bold), 2001
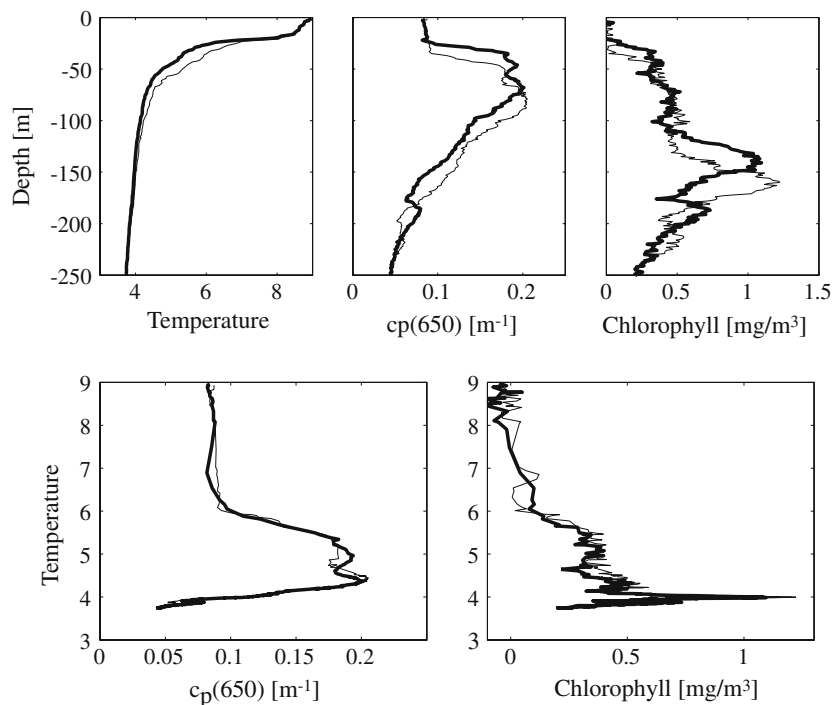
Results

Spatial and temporal variability in particulate properties

The profiles of particulate properties in June vary strongly between the 2 days of sampling (Figs. 3, 4). This variability is mostly due to the activity of large internal waves (amplitude >20 m) set up by a storm that passed by a day prior to sampling. When plotted against temperature, both chlorophyll and beam attenuation are very similar for both sampling days, indicating the (mostly) conservative behavior of these properties in the presence of internal waves over a single day.

Particulate properties vary in the water column as function of depth and differ between the June and September sampling periods (Figs. 4, 5). There does not seem to be a relation between particulate properties and stratification except for the elevated phytoplankton biomass near the surface in September. The vertical distribution of the backscattering coefficient is similar to the beam attenuation in September but not in June. The resulting change in the backscattering ratio

with depth in June, suggests a change in the bulk particulate composition with depth.

Beam-c and POC

When regressing the discrete particulate organic carbon measurements (POC, mmol C m^{-3}) and the particulate beam attenuation measurements (c_p, m^{-1}, extrapolated to 660 from measurements at 650 and 676) we find:

$$c_p(660) = POC^*0.032 - 0.024 (R^2 = 0.996).$$

This regression is similar to that found by Gunderson et al. (1998) for the Arabian Sea (0.031 and – 0.007, for slope and intercept, respectively). While the correlation coefficient is high, the confidence in the slope and intercept is low due to the 30% difference between replicate measurements of POC (we used the mean of the replicates to derive the regression). Given that large uncertainty, the regression is also consistent with data from Station Aloha near Hawaii (Fennel & Boss, 2003) and the Southern ocean (Gardner

Fig. 4 Measurements of temperature (4 casts), chlorophyll (absorption based), particulate backscattering, particulate beam attenuation, backscattering ratio, and the spectral slope of beam attenuation at St. 13 on June 28 (thin) and June 29 (bold), 2001. Two of the four temperature casts and the chlorophyll and beam attenuation data are the same as those in Fig. 3
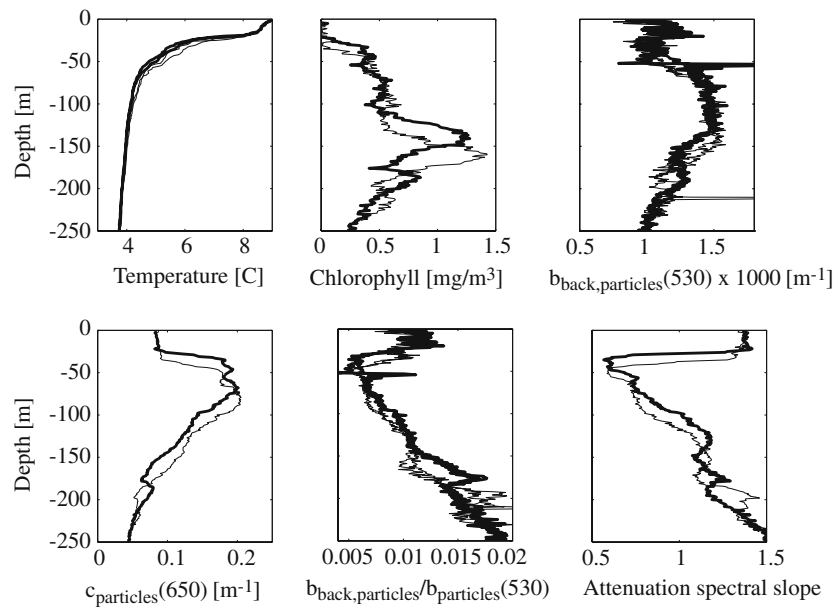
et al., 2000) where the slopes were found to be $O(0.02[m^{-1} (mmol\ C\ m^{-3})^{-1}])$.

Chlorophyll versus biomass

In both sampling periods we observed chlorophyll and particulate attenuation to be decoupled. Similar decoupling between phytoplankton bio-volume and chlorophyll has been observed in past measurements in Crater Lake (McIntire et al., 1996: Fig. 5). The decoupling is due to phytoplankton photo-acclimation, which is characterized by a typical nearly exponential increase in the chlorophyll/c_p ratio and the ratio of chlorophyll/phytoplankton-bio-volume from the surface down to the chlorophyll maximum (e.g., Kitchen & Zaneveld, 1990; Fennel & Boss, 2003: Fig. 7). This relationship is discussed in more depth in Fennel & Boss (2003), and illustrates the problem associated with using chlorophyll as a proxy phytoplankton biomass when analyzing vertical profiles.

Contribution of sub-micron particles

Sub-micron particles are found to contribute nearly 30% of chlorophyll at the chlorophyll maximum in September (Fig. 5), though their contribution to absorption or attenuation is less than 20%. Flow-cytometric analysis of samples from the lake (Sherr & Sherr, personal communication, 2002) indicates that the phytoplankton sampled on the same day are neither *Synechococcus* nor *Prochlorococcus*, the dominating sub-micron nano-phytoplankton in the oceans (based on fluorescence and scattering characteristics). We currently do not know the taxonomy of these sub-micron particles that are observed to contribute significantly to the optical properties of Crate Lake. McIntire et al. (1996) observed the presence of several species of picoplankton with diameters on the order of 1 μm but could not identify microscopically smaller cells.

Size distribution

Changes in the slope of the beam attenuation between June and September are consistent with, in general, smaller particle size in September than in June, except right next to the surface. This is consistent with the surface waters at Crater Lake being regularly dominated by the relatively large and elongated (about 70 μm long and a few micron wide) diatom *Nitzschia gracilis* in August and September (McIntire et al., 1996). In both sampling seasons, the chlorophyll maximum region is dominated by particles with a similar size distribution (c_p slope ~1).
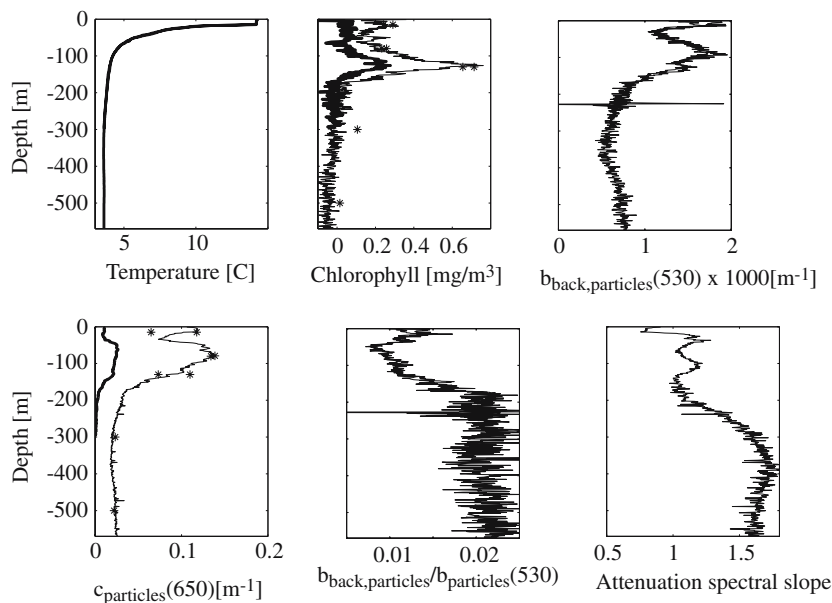
Fig. 5 Measurements of temperature, chlorophyll (absorption based), particulate backscattering, particulate beam attenuation, particulate backscattering ratio, and the spectral slope of particulate beam attenuation at St. 13 on Sep 19, 2001. The thin line represents total particulate measurements while the bold line represents the fraction smaller than 1 μm. Stars represent discrete chlorophyll-*a* (HPLC) and POC measurements. HydroScat-6 backscattering is denoted by a black line and extends only to 300 m. Eco-VSF backscattering is denoted in gray

Particulate composition and their bulk index of refraction

Sampling in June near the caldera's wall, in waters fed to the lake by a tributary, reveals a level of particulate attenuation nearly five times higher than that found near the surface at St. 13. These waters are dominated by particulate material (Fig. 6) with a ratio of particulate scattering to particulate attenuation greater than 0.93. This material has a backscattering ratio greater than 0.017 and a beam attenuation slope of nearly 1.2. Based on the analysis of Twardowski et al. (2001; Fig. 7 here) this is likely to be inorganic material, characteristic of clay minerals. This material is likely contributing to the relatively high backscattering ratio observed for the surface waters and the waters below the chlorophyll maxima at St. 13 (Fig. 7). At 50 m, however, the water of St. 13 has a backscattering ratio characteristic of organic material such as phytoplankton (0.005).

The bulk index of refraction at St. 13 in September is found to be low (< 1.1) consistent with organic, phytoplankton, and detritus (Fig. 7). The particles with the highest index of refraction are located below 200 m. This may be due to a mix of detrital particles (e.g., inorganic phytoplankton shells, small inorganic particles) and heterotrophic organisms. The variability in estimated PSD slope and index of refraction the full water column of Crater Lake is indicative of the different assemblages of particles that occupy different depths of the lake.

Colored dissolved material and DOM

Absorption by dissolved material at 440 nm increases monotonically with depth in June while having a subsurface maximum at 130 m in September (Fig. 8). Between June and September it increases mostly between 100 m and 300 m, below the layer of maximum attenuation (maximum POC and phytoplankton biomass), and in

Fig. 6 Spectra of particulate attenuation (c_p), particulate scattering (b_p), particulate absorption (a_p), dissolved absorption (a_{CDM}) and particulate backscattering (b_{bp}, multiplied by 50) averaged over 1 m at a station near the edge of the caldera where a stream entered into the lake on June 28, 2001 (black lines). Highest values were measured closest to the bottom and decreased monotonically towards the surface. Gray lines denote the same properties in the upper 10 m at the center of the lake (st. 13)
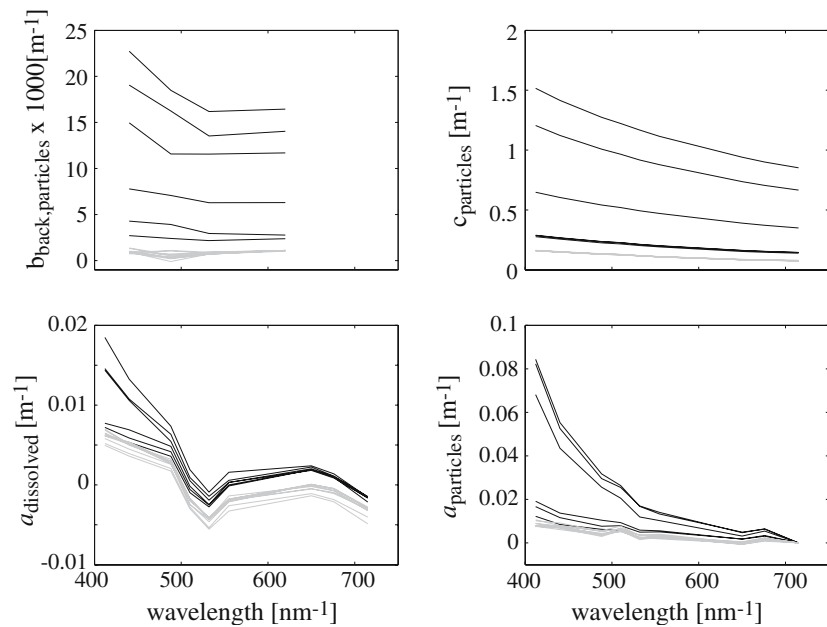
the area of maximum particulate gradient. The observed accumulation is consistent with a release of dissolved organic material as a by-product of primary and secondary production within the water column and near the bottom (where a slight increase in CDM is also observed). The dissolved absorption measured near the tributary in June is similar in magnitude to that at the center of the lake (Fig. 6), implying that no significant colored dissolved material (and by conjunction no significant amount of dissolved material) is input into the lake from the caldera's rim at that location. Unfortunately, large uncertainties in CDM values (± 0.0035 m^{-1}) did not allow us to compute a reliable CDM spectral slope (e.g., spectra in Fig. 6).

Past measurements of total organic carbon (TOC) at Crater Lake suggest a background value of about 0.1 g C m^{-3}, dominated by dissolved organic carbon (DOC) (Urbach et al., 2001; Hargreaves et al., 2007). This magnitude of DOC is at least a factor of five lower than open ocean values (compared to values found in the Bermuda Atlantic and the Hawaiian Ocean time series). For an absorption value of 0.01 ± 0.003 m^{-1} at 440 nm (Fig. 8) it implies a DOC specific absorption coefficient of

0.001 ± 0.0005 m^2 (g C)$^{-1}$. This value of the CDM specific absorption is very low and similar to values measured for marine humic acid (Blough & Green, 1995).
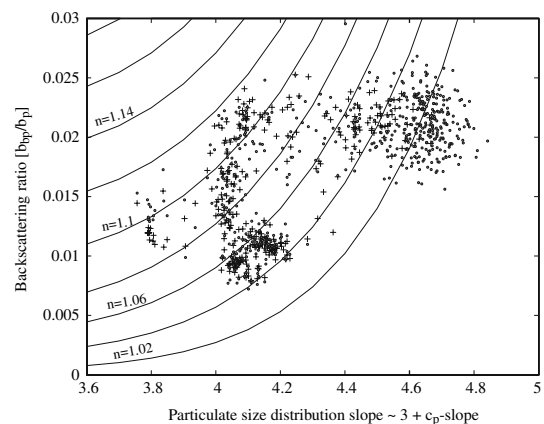

Fig. 7 Diagram depicting the backscattering-ratio against the estimated slope of the particulate size distribution (computed as 3 + spectral slope of c_p) for profile data collected at St. 13, Sep. 19 2001. Contours represent lines of equal index of refraction (n) based on Mie theory (see Twardowski et al., 2001; Boss et al., 2004). The +-sign denotes the backscattering ratio based on measurements with the HS-6 for the upper 300 m, while the dots denote the backscattering ratio based on the Eco-VSF, both at 530 nm. Low values of the bulk index of refraction (1.02–1.1) imply dominance by organic material
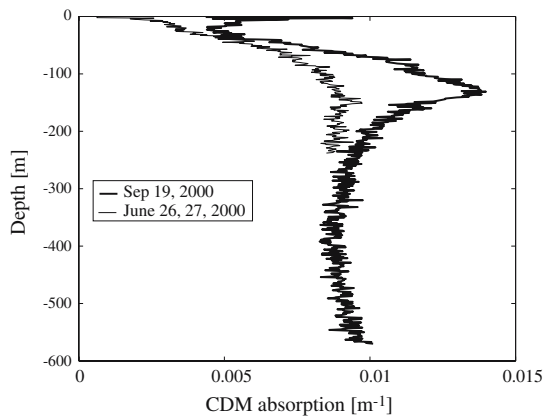
Fig. 8 Distribution of absorption by colored dissolved material at 440 nm in June (thin) and September (bold) 2001. The June profile is an average of the profiles measured on both days (28 and 29 June). Note that the uncertainty in the CDM measurement is 0.0035 m^{-1}, which is large compared to measurement (see Methods section)

Discussion

We find modern optical sensors to perform well despite the clarity of Crater Lake. These sensors provide us with high vertical resolution measurements of optical proxies of biogeochemical variables, which cannot be achieved using standard techniques.

The picture that emerges from the measurements is that the waters of Carter Lake are highly stratified optically in June and September at depths where density stratification is weak. Large amplitude internal waves were observed and may provide an important mechanism for bringing nutrients closer to the surface. Photo-acclimation in phytoplankton causes a decorrelation of the particulate beam attenuation (and also POC and phytoplankton bio-volume) and chlorophyll concentration; Chlorophyll exhibits a maximum 40–50 m deeper than that of POC.

Interestingly, optical estimates and vertical distribution of POC, and chlorophyll compare well with the relationships and distributions observed in open ocean environments. In addition, the specific absorption of CDM is found comparable to that of oceanic humic materials. These similarities suggest that biogeochemical lake studies may be relevant for understanding oceanic processes.

Sub-micron particles are found to contribute significantly to the chlorophyll concentration. To this date we do not know what are the organisms dominating this fraction in Crater Lake (McIntire, 2002, personal communication). CDM absorption, a proxy for dissolved organic material, is found to increase from spring to fall, most likely a by-product of primary and secondary production.

The instruments we have used for this study lend themselves to autonomous deployment on moorings. We strongly encourage such deployment in Crater Lake and similar environments to obtain measurements of biogeochemical proxies with high temporal resolution. Such deployments will allow the study of the lake response to forcing varying from episodic events to climate change. Real-time broadcast of the data can be used for adaptive sampling, where field sampling is driven by observed changes in the lake hydrographic and optical properties.

References

Bishop, J. K. B., 1999. Transmissometer measurement of POC. Deep-Sea Research I 46: 353–369.

Blough, N. V. & S. A. Green, 1995. Spectroscopic characterization and remote sensing of non living organic matter. In Zepp R. G. & C. Sonntag (eds), The Role of Non-living Organic Matter in the Earth's Carbon Cycle. Willey, Chichester: 23–45.

Boss, E. & W. S. Pegau, 2001. The relationship of light scattering at an angle in the backward direction to the backscattering coefficient. Applied Optics 40: 5503–5507.

Boss, E., W. S. Pegau, W. D. Gardner, J. R. V. Zaneveld, A. H. Barnard, M. S. Twardowski, G. C. Chang & T. D. Dickey, 2001a. The spectral particulate attenuation and particle size distribution in the bottom boundary layer of a continental shelf. Journal of Geophysical Research 106: 9509–9516.

Boss, E., M. S. Twardowski & S. Herring, 2001b. The shape of the particulate beam attenuation spectrum and its relaton to the size distribution of oceanic particles. Applied Optics 40: 4885–4893.

Boss, E., W. S. Pegau, M. Lee, M. S. Twardowski, E. Shybanov, G. Korotaev & F. Baratange, 2004. The particulate backscattering ratio at LEO 15 and its use to study particles composition and distribution. Journal of Geophysical Research 109, C0101410.1029/2002JC001514.

Bricaud, A., M. Babin, A. Morel & H. Claustre, 1995. Variability in the chlorophyll-specific absorption coefficients of natural phytoplankton: analysis and parameterization. Journal of Geophysical Research (C – Oceans) 100: 13,321–13,332.

Bukata, R. P., J. H. Jerome, K. Y. Kondratyev & D. V. Pozdnyakov, 1995. Optical Properties and Remote Sensing of Inland and Coastal Waters. CRC Press, Boca Raton, Florida.

Davis, R. F., C. C. Moore, J. R. V. Zaneveld & J. M. Napp, 1997. Reducing the effects of fouling on chlorophyll estimates derived from long-term deployments of optical instruments. Journal of Geophysical Research 102: 5851–5855.

Fennel, K. & E. Boss, 2003. Subsurface maxima of phytoplankton and chlorophyll—steady state solutions from a simple model. Limnology and Oceanography 48: 1521–1534.

Gardner, W. D., M. J. Richardson & W. O. Smith, 2000. Seasonal patterns of water column particulate organic carbon and fluxes in the Ross Sea, Antarctica. Deep-Sea Research II 47: 3423–3449.

Gordon, H. R., O. B. Brown, R. E. Evans, J. W. Brown, R. C. Smith, K. C. Baker & D. C. Clark, 1988. A semianalytic model of ocean color. Journal of Geophysical Research 96: 10909–10924.

Gunderson, J. S., W. D. Gardner, M. J. Richardson & I. D. Walsh, 1998. Effects of monsoons on the seasonal and spatial distribution of POC and chlorophyll in the Arabian Sea. Deep-Sea Research II 45: 2103–2132.

Hargreaves, B. R., S. F. Gardiner, M. W. Buktenica, R. W. Collier, E. Urbach & G. L. Larson, 2007. Ultraviolet radiation and bio-optics in Crater Lake, Oregon. Hydrobiologia 574: 107–140.

Kitchen, J. C. & J. R. Zaneveld, 1990. On the noncorrelation of the vertical structure of light scattering and chlorophyll *a* in case I waters. Journal of Geophysical Research 95: 20237–20246.

Klimasauskas, E., C. Bacon & J. Alexander, 2002. Mount Mazama and Crater Lake: Growth and Destruction of a Cascade Volcano U.S. Geological Survey Fact Sheet 092-02.

Maffione, R. A. & D. R. Dana, 1997. Instruments and methods for measuring the backward-scattering coefficient of ocean waters. Applied Optics 36: 6057–6067.

McIntire, C. D., G. L. Larson, R. E. Truitt & M. K. Debacon, 1996. Taxonomic structure and productivity of phytoplankton assemblages in Crater Lake, Oregon. Journal of Lake and Reservoir Management 12: 259–280.

Mobley, C. D., 1994. Light and Water: Radiative Transfer in Natural Waters. Academic Press, San Diego.

Moore, C., E. J. Bruce, W. S. Pegau & A. D. Weideman, 1997. WET Labs ac-9: field calibration protocol, deployment techniques, data processing, and design improvements. ''Ocean Optics XII'', Proceedings of the Society of Photo Optics Instrumentation Engineers 2963: 725–730.

Morel, A., 1973. Diffusion de la lumiere par les eaux de mer. Resultat experimentaux et approch theorique. In Agard Lecture Series 61 on Optics of the Sea~ Advisory Group for Aerospace Research and Development; NATO, London: 3.1.1–76.

Morel, A., 1974. Optical properties of pure water and pure sea water. In Jerlov, N. G. & E. S. Nielsen (eds), Optical Aspects of Oceanography. Academic Press, NewYork.

Pettit, E., 1936. On the color of Crate Lake water. Proceedings, National Academy of Science 22: 139–146.

Smith, R. C. & K. S. Baker, 1981. Optical properties of the clearest natural waters (200–800 nm). Applied Optics 20: 177–184.

Sosik, H. M. & B. G. Mitchell, 1995. Light absorption by phytoplankton, photosynthetic pigments and detritus in the California Current System. Deep Sea Research 42: 1717–1728.

Spinrad, R. W. & J. R. V. Zaneveld, 1982. An analysis of the optical features of the near-bottom and bottom nepheloid layers in the area of the Scotian Rise. Journal of Geophysical Research 87: 9553–9561.

Twardowski, M. S., J. M. Sullivan, P. L. Donaghay & J. R. V. Zaneveld, 1999. Microscale quantification of the absorption by dissolved and particulate material in coastal waters with an ac-9. Journal of Atmospheric Oceanic Technology 16: 691–707.

Twardowski, M. S., E. Boss, J. B. Macdonald, W. S. Pegau, A. H. Barnard & J. R. V. Zaneveld, 2001. A model for estimating bulk refractive index from the optical backscattering ratio and the implications for understanding particle composition in Case I and Case II waters. Journal of Geophysical Research 106: 14129–14142.

Urbach, E., K. L. Vergin, L. Young, A. Morse, G. L. Larson & S. J. Giovannoni, 2001. Unusual bacterioplankton community structure in ultra-oligotrophic Crater Lake. Limnology and Oceanography 46: 557–572.

Zaneveld, J. R. V., J. C. Kitchen & C. C. Moore, 1994. Scattering error correction of reflecting tube absorption meters. In Ackleson, S. (ed.), Ocean Optics XII, Proc. SPIE 2258: 44–55.

Zaneveld, J. R. V., S. Pegau & J. L. Mueller, 2003. Volume scattering function and backscattering coefficients: instruments, characterization, field measurements and data analysis protocols. In Mueller, J. L., G. S. Fargion & C. R. McClain (eds.), Ocean Optics Protocols for Satellite Ocean Color Sensor Validation, Revision 4, Volume IV: Inherent Optical Properties: Instruments, Characterizations, Field Measurements and Data Analysis Protocols, NASA Tech. Memo., 2003-211621/Rev4-Vol.IV. Greenbelt: NASA Goddard Space Flight Center: 65–76.